



Characterization, sources and risk assessment of PM_{2.5}-bound polycyclic aromatic hydrocarbons (PAHs) and nitrated PAHs (NPAHs) in Harbin, a cold city in Northern China

Lixin Ma^a, Bo Li^a, Yuping Liu^b, Xiazhong Sun^a, Donglei Fu^a, Shaojing Sun^a, Samit Thapa^a, Jialu Geng^a, Hong Qi^{a,c,*}, Anping Zhang^d, Chongguo Tian^{e,**}

^a School of Environment, Harbin Institute of Technology, Harbin 150090, PR China

^b Heilongjiang Provincial Environmental Science Research Institute, Harbin 150090, China

^c State Key Laboratory of Urban Water Resource and Environment, Harbin Institute of Technology, Harbin 150090, China

^d College of Environment, Zhejiang University of Technology, Hangzhou 310014, China

^e Key Laboratory of Coastal Environmental Processes and Ecological Remediation, Yantai Institute of Coastal Zone Research, Chinese Academy of Sciences, Yantai 264003, China

ARTICLE INFO

Article history:

Received 3 December 2019

Received in revised form

8 April 2020

Accepted 11 April 2020

Available online 15 April 2020

Handling editor: Prof. Jiri Jaromir Klemes

Keywords:

PM_{2.5}

Polycyclic aromatic hydrocarbons (PAHs)

Nitrated PAHs (NPAHs)

Source apportionment

Risk assessment

ABSTRACT

Inhalation of atmospheric particulates is an significant way for polycyclic aromatic hydrocarbons (PAHs) and substituted PAHs (SPAHS) to enter the human lungs. Some SPAHS are more virulent than parent PAHs. Atmospheric fine particulate matter (PM_{2.5}) samples were obtained at Harbin Institute of Technology (HIT) in Harbin, China. This study provided the first description, source apportionment, and health risk for PM_{2.5}-bound 16 PAHs and 16 nitrated PAHs (NPAHs) in cold regions of China. On average, the PM_{2.5}, PM_{2.5}-bound PAHs and NPAHs concentrations were 80.8 μg/m³, 86.9 ng/m³ and 5.48 ng/m³. Significant increases in PM_{2.5} (274 μg/m³) and PM_{2.5}-bound NPAHs (24.7 ng/m³) concentrations were measured during the straw burning in autumn, while the concentration of PM_{2.5}-bound PAHs (215 ng/m³) increased obviously in winter. Source apportionment showed that the main source of PAHs was combustion, while besides direct emissions, about 20% of NPAHs came from the secondary formation. Controlling coal combustion and biomass burning might be an effective measure to improve air quality during the heating period in Harbin. The influence of meteorological conditions on PAHs and NPAHs concentration indicated that pollutants were more susceptible to meteorological conditions during the heating period than during the non-heating period, especially for PAHs. The health risk analysis indicated that the highest health risk caused by exposure to the PM_{2.5}-bound PAHs and NPAHs was in winter, and this was inconsistent with the trend of PM_{2.5} pollution. Cancer risk assessments demonstrated the potential cancer risk at this PAHs and NPAHs concentration level.

© 2020 Elsevier Ltd. All rights reserved.

1. Introduction

Air pollution in cities has related to increased rates of morbidity and mortality in many countries (Samet et al., 2000). For annual premature mortality, air pollution is regarded as one of the largest causes (Egide et al., 2018). Air pollution with significant regional characteristics was associated with the local emission sources, meteorological conditions, geographical features, population

density, architectural patterns and lifestyle. The most representative indicator to assess the air quality in an area is the concentration of ambient particulate matter (PM) which can be deposited into the respiratory system to result in cardiovascular disease (Querol et al., 2004), respiratory disease (Mabahwi et al., 2014), and lung cancer (Sarigiannis et al., 2015), etc. Fine particles (PM_{2.5}, aerodynamic particle diameter less than 2.5 μm) can enter the lungs and circulate through the blood (Chitranshi et al., 2015), and are of concern because of its strong adsorption (Yin and Xu, 2018).

The adsorption of PAHs with carcinogenic, teratogenic and mutagenicity significantly increases the toxicity of PM_{2.5}, which is even higher than health risk currently recognized due to PAHs can produce more toxic derivatives through a series of chemical reactions (Santos et al., 2018). For example, NPAHs, derivatives of

* Corresponding author. State Key Laboratory of Urban Water Resource and Environment, Harbin Institute of Technology, 73 Huanghe Road, Nangang District, Harbin, Heilongjiang, 150090, China.

** Corresponding author.

E-mail addresses: hongqi@hit.edu.cn (H. Qi), cgtian@yic.ac.cn (C. Tian).

PAHs, its carcinogenicity and direct-acting mutagenicity are one and five orders of magnitude higher than their parent PAHs, respectively, although to exist at concentrations one to three magnitudes lower than those of PAHs (Nassar et al., 2011).

PM_{2.5} is mainly contributed by direct emission including traffic exhaust, industrial processes and secondary reaction. Parent PAHs are mainly contributed by incomplete combustion processes. For NPAHs, except direct emissions, high levels of atmospheric oxidants (hydroxyl radicals, nitrate radicals and ozone) can initiate the transformation of parent PAHs into their derivatives (Zimmermann et al., 2013). For instance, 1-nitropyrene (1-NP) and 7-nitrobenz[a]anthracene (7-NBaA) had been identified in diesel particles (Albinet et al., 2007), while 2-nitrofluoranthene (2-NF) and 2-nitropyrene (2-NP) can be formed from the reactions of gas-phase radicals with fluoranthene (Fla) and pyrene (Pyr), respectively (Jariyasopit et al., 2014). 9-Nitroanthracene (9-NA) can be formed from both direct emission and atmospheric reactions (Albinet et al., 2007). These compounds can be used as source indicators.

In China, related studies on PAHs and its derivatives in PM_{2.5} mainly in some central cities with high population density, serious pollution caused by rapid industrial, manufactural and commercial development. It has been reported that PM_{2.5}-bound NPAHs and OPAHs in Beijing accounted for 8% of parent PAHs during the Beijing Olympic Games. PAHs were related to local and regional emissions, while its derivatives (NPAHs and OPAHs) were mainly related to local emissions (Wang et al., 2011). It has been reported that the secondary formation had a significant contribution to NPAHs concentrations in Jinan, especially in winter (Li et al., 2019). However, relatively few studies were conducted in cold northern cities, in particular, there have been no studies on PAHs derivatives. The results from this work could provide important information for further relevant studies in this region.

Harbin, as a typical industrial city in northern China, is characterized by greater population density, dense traffic, huge industrial coal consumption, complex industrial structure and wide annual temperature range (up to 60 °C) resulting in the heating period accounting for half the year. For instance, Harbin's total area is 3.20 times that of Beijing, but its coal consumption in 2017 was 4.61 times that of Beijing, indicating that Harbin has considerable coal consumption. Due to a large amount of biomass burning for cooking and heating in the neighboring regions and frequent inversion in the cold season, Harbin has become one of the cities with the most serious PM_{2.5} pollution in China and continually resulted in haze in recent winters. It is urgent to identify the pollution sources and establish control measures of these pollutants to improve the air quality in Harbin.

In this study, PM_{2.5} samples at the second campus of the Harbin Institute of Technology (HIT) were collected and monitored. PM_{2.5}-bound 16 PAHs and 16 NPAHs were quantified. The major aims of this work were as follows: (1) to determine levels, temporal variation and composition of PM_{2.5}-bound PAHs and NPAHs in Harbin. (2) to explore the influence of meteorological conditions on PAHs and NPAHs. (3) to identify the possible sources and distribution of pollution sources of PAHs and NPAHs. (4) to assess health risks exposed to PAHs and NPAHs.

2. Methodology

2.1. Study sites and sampling

Harbin, like the typical cold and industrial area in China, is the most densely populated city in northeast China, with 9.95 million inhabitants. It has a typical monsoon-influenced subtropical climate with annual temperature range above 60 °C and half the

time of a year in the heating period (from mid-October to mid-April of the following year). With the rapid development of urbanization leads to increased coal consumption, which has caused severe air pollution in recent years.

PM_{2.5} 24-h samples were collected (from 7:00 a.m. to 7:00 a.m. of the following day) on the rooftop of the school of the environment at the second campus of HIT (45°45'N, 126°40'E, ~12 m above the ground) (Fig. S1). The sampling was carried out in the commercial area and was an ideal location for studying air pollution because there was no obvious point pollution source. The high volume (1005 L/min) suspended particle sampler (Model: TH-150A; Wuhan Tianhong Company, China) was used to obtain samples onto quartz microfibre filters (20 × 25 cm) prebaked for 6 h at 600 °C to remove organic contaminants. Among 82 PM_{2.5} samples collected (from June 2017 to May 2018), 22, 15, 24 and 21 were obtained in spring, summer, autumn and winter, respectively. Samples were stored in a refrigerator at -20 °C before analysis. During the sampling period, hourly meteorological data (wind speed, mixed layer height, temperature, surface pressure, daily rainfall, solar radiation, relative humidity) were simulated by Weather Research and Forecasting with Chemistry model (WRF-Chem), and atmospheric pollutants (SO₂, NO₂, CO, O₃, PM_{2.5} and PM₁₀) data came from the Hongqi street environmental monitoring station near the sampling site.

2.2. Sample analysis

The filters were placed in 34 mL extraction cells which successively added 3 g anhydrous sodium sulfates and diatomaceous earth to about two-thirds of the extraction cells volume, and spiked with a mixture of three deuterated-PAHs (Naphthalene-D8, Fluorene-D10, Pyrene-D10) and three deuterated-NPAHs (2-Nitrofluorene-D9, 9-Nitroanthracene-D9 and 6-Nitrochrysene-D11) as surrogate standards for the PAHs and NPAHs, respectively. Each filter was extracted twice using pressurized liquid extraction with hexane and acetone (1:1, v/v). For chemical analysis, the extracts were purified and eluted. The eluted fractions were concentrated to about 1 mL and were dissolved in isoctane. The pollutants measured in this work are shown in Table 1.

16 PAHs were analyzed using Agilent 6890NGC and 5973MS in selected ion monitoring (SIM) mode. Chromatographic column: HP-5MS (30 m × 0.25 mm × 0.25 μm). Ion source: electron impact ionization (EI). The injected volume was 1 μL in splitless mode. Column flow: 0.6 mL/min. The oven temperature program: held at 80 °C for 3 min, heat to 200 °C (10 °C/min) and held for 4 min, then heat to 300 °C (6 °C/min) and held for 8 min.

16 NPAHs were detected using an Agilent 7000A GC/MS Triple Quadrupole System (Agilent Technologies Inc, USA) and quantitatively analyzed in MRM mode. Ion source: inert ion source (EI). Chromatographic column: Agilent 19091J-433 HP-5 (30 m × 0.25 mm × 0.25 μm); . The oven temperature program: 80 °C ramp to 240 °C (20 °C/min) and held for 7.5 min, then ramp to 300 °C (30 °C/min) and held for 2.5 min.

2.3. Data analysis

2.3.1. Diagnostic ratios

Based on the fact that certain individual PAHs and NPAHs may be emitted from specific sources (Ravindra et al., 2008), including coal, firewood, gasoline, diesel, and natural gas, the ratios of a certain particular compound can be used as source indicators. There have been many studies on the sources of PAHs and their derivatives by using diagnostic ratios (Yin and Xu, 2018). The ratios of 11 groups of characteristic molecules and corresponding pollution sources used in this study were displayed in supplementary file Table S1.

Table 1
Parent PAHs and NPAHs (and their abbreviations) measured in this study.

no. PAHs	compound	abbreviation	no. NPAHs	compound	abbreviation
1	Naphthalene	Nap	1	1-Nitronaphthalene	1-NN
2	Acenaphthylene	Acy	2	2-Nitronaphthalene	2-NN
3	Acenaphthene	Ace	3	1,5-Dinitronaphthalene	1,5-DNN
4	Fluorene	Fl	4	1,3-Dinitronaphthalene	1,3-DNN
5	Phenanthrene	Phe	5	1,8-Dinitronaphthalene	1,8-DNN
6	Anthracene	Ant	6	5-Nitroacenaphthene	5-NAce
7	Fluoranthene	Fla	7	2-Nitrofluorene	2-NFLo
8	Pyrene	Pyr	8	3-Nitrophenanthrene	3-NPhe
9	Benzo(a)anthracene	BaA	9	9-Nitrophenanthrene	9-NPhe
10	Chrysene	Chr	10	2-Nitroanthracene	2-NA
11	Benzo(b)fluoranthene	BbF	11	9-Nitroanthracene	9-NA
12	Benzo(k)fluoranthene	BkF	12	9,10-Dinitroanthracene	9,10-DNA
13	Benzo(a)pyrene	BaP	13	3-Nitrofluoranthrene	3-NF
14	Indeno(1,2,3-c,d)pyrene	IDP	14	1-Nitropyrene	1-NP
15	Dibenzo(a,h)anthracene	DBahA	15	6-Nitrochrysene	6-NChr
16	Benzo(g,h,i)perylene	Bghip	16	7-Nitrobenz[a]anthracene	7-NBaA

2.3.2. Positive matrix factorization (PMF)

PMF 5.0 model was used to analyze the sources of contaminants. The calculation of the uncertainty (Unc) required to initiate the model can be divided into two cases. When the concentration is less than or equal to the method detection limit (MDL), the Unc was calculated by Eq. (1):

$$\text{Unc} = 5/6 \times \text{MDL} \quad (1)$$

When the concentration is greater than the provided MDL, the Unc was calculated by Eq. (2):

$$\text{Unc} = \left[(\text{Error fraction} \times \text{concentration})^2 + (0.5 \times \text{MDL})^2 \right]^{1/2} \quad (2)$$

2.3.3. Potential source contribution function (PSCF)

The PSCF is used to calculate the probability of occurrence of specific airflow in the ij -th cell, which can reflect the distribution of atmospheric pollution sources. The principles and calculations have been described in detail in previous reports and will not be covered in this work (Li et al., 2019).

In this work, the standard value of PAHs (86.9 ng/m³) and NPAHs (1.78 ng/m³) were set as the median of its concentration. The resolution of the model is 1° × 1°, and the simulated height was 1000 m. The 3-day back trajectory every 6 h was calculated using the Hybrid single-particle Lagrangian Integrated Trajectory (HYSPPLIT) model. In order to reduce the influence of small $n(i,j)$ value on the uncertainty of these cell values, PSCF value was multiplied by weight function W_{ij} . The values of W_{ij} were as follows: if $n_{ij} > 15$, $W_{ij} = 1$; if $7 < n_{ij} \leq 15$, $W_{ij} = 0.7$; if $4 < n_{ij} \leq 7$, $W_{ij} = 0.42$; if $0 < n_{ij} \leq 4$, $W_{ij} = 0.17$.

2.3.4. Risk assessment

According to the exposure assessment, the potential health impacts of exposure to PM_{2.5}-bound PAHs and NPAHs can be expressed by the total carcinogenic equivalent toxicity (Σ TEQ), total mutagenic equivalent toxicity (Σ MEQ), non-carcinogenic risk (non-CR), incremental lifetime cancer risk (ILCR) and loss of life expectancy (LLE). Given that receptors have different physiological characteristics and living habits due to differences in age and gender, this study divided receptors into children (1–11 years old), adolescents (12–17 years old) and adults (18–70 years old), and

differentiated them by gender. Detailed information on the Σ TEQ, Σ MEQ, non-CR, ILCR and LLE calculations is described in Text S1.

2.4. Quality control and quality assurance

The detection limits of the method were 0.0180–0.0774 ng/m³ for PAHs and 0.0133–0.486 pg/m³ for NPAHs. The average recoveries were 87–105% for PAHs and 93–124% for NPAHs. The recoveries of PAHs and NPAHs surrogates were determined.

Before sample extraction and analysis, substitutes are added to the extraction cells to monitor the whole analysis process. The recoveries of 6 spiked perdeuterated surrogates were: Naphthalene-D8: 86–98%, Fluorene-D10: 94–110%, Pyrene-D10: 93–115%, 2-Nitrofluorene-D9: 95–115%, 9-Nitroanthracene-D9: 92–119% and 6-Nitrochrysene-D11: 102–115%. Process blank, laboratory blank and field blank were analyzed, and the measured values of PAHs and NPAHs could be ignored. Actual sample monitoring results were not corrected by the blank and internal standard recovery. Repeated samples were analyzed by the above mentioned, and the average variance was 9%.

3. Results and discussion

3.1. Concentration of the PM_{2.5}

The annual concentration of PM_{2.5} monitored by air quality monitoring station was 80.8 μg/m³ (CMISS-China Meteorological Data Service Center, 2005), which was 2.31 and 8.08 times of the annual average exposure limit of 35 μg/m³ for China and the annual average exposure limit of 10 μg/m³ for world health organization (WHO), respectively. This indicated a severe PM_{2.5}-polluted environment in Harbin.

In this study, the selected PM_{2.5} samples from June 2017 to May 2018 were collected by the active sampler, with a total of 82 samples, including 22 samples in spring, 15 samples in summer, 24 samples in autumn and 21 samples in winter. The temporal variation of PM_{2.5} concentrations is shown in Fig. S2. Among the 82 samples collected, the annual average concentration of PM_{2.5} was 141 μg/m³. The highest mass concentration of PM_{2.5} was measured in autumn (188 μg/m³), followed by spring (144 μg/m³), winter (124 μg/m³), and summer (82.1 μg/m³). The highest concentration in autumn was most likely associated with the start of heating and straw burning, while the lowest concentration in summer was consistent with the absence of combustion sources and favorable diffusion conditions.

According to the *t*-test, the concentrations of PM_{2.5} in summer were significantly different from the other three seasons ($P < 0.05$), and there were no significant differences among spring, autumn and winter ($P > 0.05$), indicating that the source of PM_{2.5} in summer might be different from the other three seasons. PM_{2.5} concentrations during the heating and non-heating periods were 167 $\mu\text{g}/\text{m}^3$ and 102 $\mu\text{g}/\text{m}^3$, respectively. This suggested that large amounts of combustion (coal and biomass) during the heating period may be important contributors to PM_{2.5}.

3.2. Evaluation of PM_{2.5}-bound PAHs and NPAHs concentrations

In this work, PAHs and NPAHs in PM_{2.5} were identified and quantified. The annual average concentration of PAHs was 86.9 ng/m^3 in Harbin. Compared with other countries and regions, such as Portugal (9.11 ng/m^3) (Slezakova et al., 2013) and Germany (1.34 ng/m^3) (Pietrogrande et al., 2011) in Europe, the United States (3.0 ng/m^3) (Sevimoglu and Rogge, 2016) and Mexico (2.92 ng/m^3) (Mugica-Alvarez et al., 2015) in the Americas, and India (40 ng/m^3) (Rajput et al., 2011) in Asia, the concentrations of PM_{2.5}-bound PAHs in Harbin were higher. Compared with other cities in China, the concentrations of PAHs in Harbin were significantly higher than that in Beijing (53.8 ng/m^3) (Lin et al., 2015) and in Hong Kong (4.59 ng/m^3) (Ma et al., 2016), but lower than in Zhengzhou (111 ng/m^3) (Wang et al., 2014) (Table S4).

Fig. 1a shows the temporal variations of PAHs concentrations. Considering the strong carcinogenic PAHs compound, BaP, its concentration (2.63 ng/m^3 in spring, 4.92 ng/m^3 in autumn and 14.3 ng/m^3 in winter) all exceed the China Air Quality Standard (AQS; GB3095-2012) limit of BaP in inhalable particles (2.5 ng/m^3) except for summer samples (0.422 ng/m^3 in summer). The highest concentration of PAHs was detected in winter (215 ng/m^3), followed by autumn (72.1 ng/m^3), spring (35.8 ng/m^3) and summer (5.88 ng/m^3). The reason for this seasonal tendency was that the heating period of residents in Harbin starts in the middle of October and ends in the middle of April the next year. In addition to the relatively low emission, the low PAHs concentration in summer might be related to the strong photodegradation reaction under high radiation conditions. It has been reported that most PAHs exposed to NO₃/N₂O₅ and O₃ radicals will degrade to some extent under photocatalytic conditions (Jariyasopit et al., 2014).

As for the derivatives of PAHs, NPAHs, its concentration in PM_{2.5} in the Harbin atmosphere was not reported before. In this work, the annual concentration of NPAHs was 5.48 ng/m^3 . Compared to the other megacities, such as Mexico (0.152 ng/m^3) (Valle-Hernández et al., 2010), Beijing, China (1.14 ng/m^3) (Lin et al., 2015), and Jinan, China (1.88 ng/m^3) (Li et al., 2019), NPAHs concentrations in Harbin were higher, indicating a more NPAHs-polluted environment. The seasonal tendency of NPAHs concentrations was different from PAHs, with the highest concentration observed during the autumn (13.8 ng/m^3), followed by winter (2.35 ng/m^3), spring (1.57 ng/m^3) and summer (1.23 ng/m^3) (Fig. 1c). The results were different from those reported that the highest concentration of NPAHs in winter (Li et al., 2019). Compared with PAHs, in addition to direct emission (straw burning and coal heating), the high temperature and solar radiation in autumn may also promote the secondary formation of NPAHs.

3.3. Molecular compositions of PAHs and NPAHs

The composition profile of PAHs and NPAHs during the sampling period is shown in Fig. 1b and d, respectively. From November to March of the next year, the sum of Pyr, Fla and Phe accounted for more than 45% (Pyr: 16.0%, Fla: 18.2% and Phe: 13.6%). Fla is predominant PAHs in the coal combustion process (Sofowote et al.,

2008), and Pyr mainly comes from the biomass burning process (Singh et al., 2013). This was consistent with the coal-burning for urban heating and a large amount of biomass burning for cooking and heating in the neighboring regions in Harbin during this period. During the hot period (from July to October), IDP and Bghip together accounted for more than 35% (IDP: 16.4% and Bghip: 19.5%). BghiP and IDP were characteristic emissions from traffic sources (Yang et al., 2013), so in addition to emissions from coal combustion, vehicle emission was also an important contributor to PAHs in Harbin. The proportion of BaP was stable throughout the year. It has been reported that BaP is related to coal combustion, so coal burning was an important source (Hanedar et al., 2014), which might be attributed to industrial coal in the study area.

As for the NPAHs, from July to September, the proportion of 9,10-DNA increased significantly, ranging from 70.0 to 78.5%. The proportion of 9-NA was relatively high, averaging 38.6% during the heating period. The results were coincident with the previous reports (Li et al., 2019). 9-NA can be produced from diesel vehicle emission and secondary reaction (Ringuet et al., 2012), while 1-NP is characteristic emissions from diesel vehicles (Ratcliff et al., 2010). Based on the significant correlation between 9-NA and 1-NP, it could be seen that both sources were similar, and diesel vehicle emission was an important contributor to NPAHs in Harbin during the heating period.

From October 27 to November 4, the sum of 3NPhe and 9NPhe accounted for a high proportion with an average of 30.8% (3-NPhe: 13.7% and 9-NPhe: 17.1%). Several reports have suggested the generation of 3-NPhe and 9-NPhe from the secondary reaction (Lin et al., 2015), which was consistent with the description in section 3.2 that high temperature and solar radiation in autumn promoted the secondary formation of NPAHs. From December to March of the next year, the percentage of 9-NPhe (15.8%) was significantly higher than that of 3-NPhe (3.18%), indicating that the two might have different secondary formation mechanisms during cold periods, which should be confirmed by further studies.

3.4. Influence of the meteorological conditions on the PAHs and NPAHs concentrations

Air pollution is affected by meteorological conditions (wind speed, mixed layer height and surface pressure), which are related to the dilution and diffusion of pollutants, and temperature and solar radiation, which contribute to the gas phase reaction process of organic compounds. For the cold areas in northern China, temperature, as the main factor affecting the amount of coal combustion for heating, can indirectly affect the emission of PAHs and NPAHs.

Table S5 lists the correlation among the concentrations of PAHs, NPAHs and meteorological conditions (wind speed, mixed layer height, temperature, surface pressure, daily rainfall, solar radiation, relative humidity) measured on the same days during the heating and non-heating periods. Most PAHs were significantly negatively correlated with the wind speed, mixed layer height, temperature and solar radiation during the heating period, while most PAHs were significantly negatively correlated with the mixed layer height, temperature, surface pressure and solar radiation during the non-heating period (Pearson correlation coefficient, $P < 0.05$). This result indicated that PAHs might be affected by the combination of diffusion and degradation. The negative correlation between PAHs and wind speed, mixed layer height during the heating period was stronger than that during the non-heating period, indicating that the adverse dilution and diffusion conditions including weak wind, frequent inversion and low mixing layer height had a greater influence on the PAHs concentrations in PM_{2.5} during the heating period. The PAHs concentration throughout the sampling period

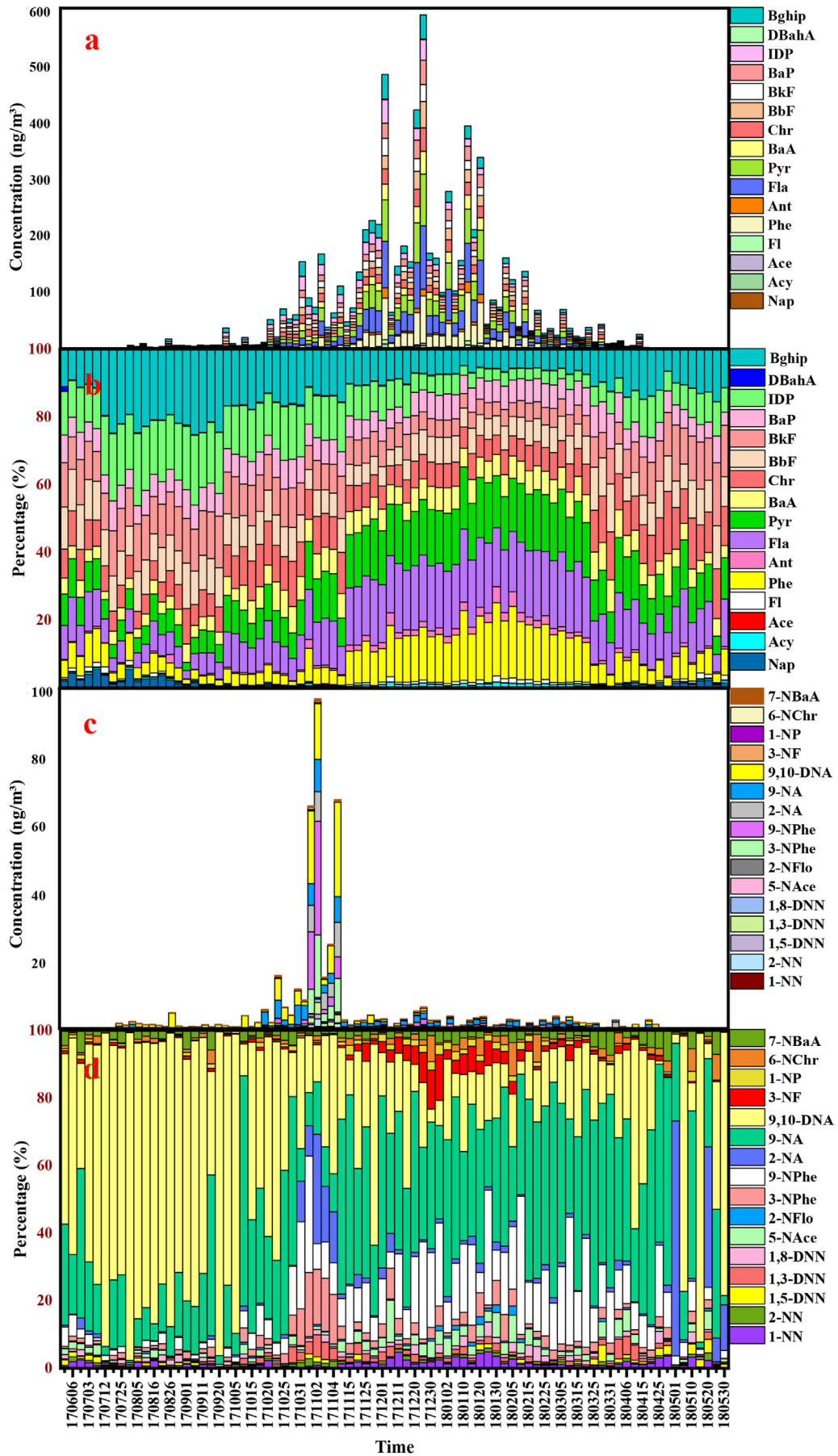


Fig. 1. Temporal variation of concentration and composition of PM_{2.5}-bound PAHs and NPAHs.

had a significant negative correlation with the temperature and solar radiation, and the PM_{2.5}-bound PAHs concentrations during the non-heating period decreased more quickly than during the heating period with an increase in the temperature and solar radiation, indicating the stronger the photochemical and oxidative degradation of PAHs during the non-heating period.

It should be noted that the correlation between NPAHs and temperature and solar radiation was opposite to that of the correlation between PAHs and temperature and solar radiation during the heating period (Fig. 2). For example, 9,10-DNA was significantly positively correlated with temperature and solar radiation, while its parent, Ant was significantly negatively correlated with temperature and solar radiation during the heating period. This might indicate the secondary formation process of NPAHs. By comparing the correlation between PAHs, NPAHs and meteorological conditions, it was found that the correlation between PAHs and meteorological conditions was stronger, indicating that PAHs were more influenced by meteorological conditions.

3.5. Sources of PAHs and NPAHs

3.5.1. Correlation of parent PAHs and NPAHs with atmospheric pollutant concentrations

Supporting file Table S6 lists the correlation of parent PAHs and NPAHs with SO₂, NO₂, CO and O₃ concentrations during the heating and non-heating periods. Most of the individual PAHs concentrations were significantly correlated with SO₂ (positive correlation) and O₃ concentrations (negative correlation) during the heating period indicating that coal combustion might be an important source. There was no correlation between PAHs and NPAHs concentrations and atmospheric pollutant concentrations during the non-heating period. The stronger positive correlation between 7 carcinogenic PAHs ($\Sigma 7\text{carcPAHs}$: BaA, Chr, BbF, BkF, BaP, IDP and DBaH) and SO₂ during the heating period indicated the possible adverse effects of coal-fired heating on human health.

3.5.2. Diagnostic ratios

The diagnostic ratios were widely employed to identify and distinguish the potential source of PAHs and NPAHs such as wood-burning, coal, gasoline, diesel, and petroleum combustion emissions, among others. The calculated results are shown in Fig. 3.

Most samples had BaP/Bghip ratios between 0.3 and 0.8 during the non-heating periods indicating gasoline and diesel engine combustion sources, while most of the samples had BaP/Bghip ratios between 0.4 and 1.2 during the heating periods pointing to mixed sources of coal combustion and diesel engine combustion (Fig. 3a). Most of the samples had BbF/BkF ratios above 0.5, implying that diesel engine combustion was an important source during the heating and non-heating periods (Fig. 3a). Most of the samples had 1-NP/Pyr ratios close to 0.001, indicating coal combustion was the main source throughout the sampling period (Fig. 3b). The 9-NA/1-NP ratios greater than 10 indicates the biomass combustion source (Chuesaard et al., 2014). All the samples have 9-NA/1-NP ratios above 10 during the heating periods, while 97.0% of 9-NA/1-NP ratios were greater than 10 (mean 34.6) during the non-heating periods (Fig. 3b).

In Fig. 3c, most of Pyr/BaP ratios were close to 1 indicating gasoline vehicle emission, and most samples have Fla/(Fla + Pyr) ratios above 0.5, implying that coal combustion was a strong contributor throughout the year. Most of the IDP/(IDP + BgP) ratios were between 0.2 and 0.5, indicating liquid fossil fuel combustion source throughout the year (Fig. 3d). BaP/(BaP + Chr) ratios equal to 0.56 and 0.65 indicate diesel and gasoline vehicle emissions, respectively (Akyüz and Çabuk, 2010), while BaP/(BaP + Chr) ratios were range from 0.441 to 1.12 (mean 0.820) during the heating

periods and 0.334 to 1.49 (mean 0.795) during the non-heating periods, so no single source was suggested (Fig. 3d). Based on the ratios of Ant/(Ant + Phe) and BaA/(BaA + Chr), the study area more likely to be contributed by pyrogenic sources during the heating period (Fig. 3e). For the non-heating period, besides the pyrogenic sources, it was also contributed by petrogenic and mixed sources (Fig. 3e).

The ratios of low ring PAHs (LPAHs: Nap, Acy, Ace, Fl, Phe, Ant, Fla, Pyr, BaA and Chr) to high ring PAHs (HPAHs: BbF, BkF, BaP, IDP, DBaH and Bghip) and NPAHs to PAHs can also reflect the source of pollution. In this study, $\Sigma\text{LPAHs}/\Sigma\text{HPAHs}$ ratios were less than 1, indicating pyrogenic sources throughout the sampling period (Fig. 3f). $\Sigma\text{NPAHs}/\Sigma\text{PAHs}$ ratios equal to 0.0001 and 0.13 indicate coal combustion and diesel engine emissions, respectively (Zhang et al., 2015). $\Sigma\text{NPAHs}/\Sigma\text{PAHs}$ ratios ranged from 0.00604 to 0.895 (mean 0.0927) during the heating periods and ranged from 0.00951 to 0.796 (mean 0.199) during the non-heating periods, so no single source was suggested (Fig. 3f).

Overall, crude source apportionment of PM_{2.5}-bound PAHs and NPAHs were qualitatively identified by the diagnostic ratios. The results showed that the study area was affected by mixed sources, including coal, diesel engine and non-fossil fuel combustion, biomass burning, vehicular emission and petrogenic source.

3.5.3. PMF

PMF model was used to apportion the possible pollution sources of PM_{2.5}-bound PAHs and NPAHs in Harbin, and source profiles are shown in Figs. S3–4. PMF-source#1 of PAHs mainly included of 3-ring PAHs. PMF-source#2 of PAHs mainly included of 5-ring and 6-ring PAHs. The profiles of PMF-source#1, PMF-source#2 and PMF-source#3 were similar to that of straw burning (Lin et al., 2015), vehicle emissions (He et al., 2008) and coal combustion, respectively (Zhang et al., 2008). Coal combustion (42.0%) and biomass burning (32.2%) were the main sources of PAHs during the heating period, while vehicle emission (38.1%) during the non-heating period was significantly higher than that during the heating period (25.7%) (Fig. S5). Of note, the contribution concentration of three sources (coal combustion, biomass burning and traffic emission) during the heating period was 12.1, 15.6 and 7.41 times of that during the non-heating period. This meant that controlling coal combustion and biomass burning, rather than transportation, might be a more effective measure to improve air quality during the heating period in Harbin.

As for NPAHs, PMF-source#1 was characterized by 3-NF (Albinet et al., 2007), 1-NN, 2-NN, 3-NPhe and 9-NPhe (Zhan et al., 2012), which was identified as secondary formation. PMF-source#2 was dominated by 9-NA, 1-NP, 6-NChr and 7-NBaA. According to the results discussed in section 3.2, 9-NA can be used as a direct emission source indicator for NPAHs in this study. It has been reported that 1-NP, 6-NChr and 7-NBaA are mainly produced by direct emission (Albinet et al., 2007). NPAHs sources were mainly attributed to direct emission contribution, with a contribution rate of more than 75% (80.8% during the heating period and 76.5% during the non-heating period). The stronger contribution of secondary formation to NPAHs during the non-heating period (23.5%) was related to the atmospheric reaction of NPAHs promoted by high temperature and solar radiation during this period (Fig. S5). This was consistent with the results discussed in section 3.4 of this study.

3.5.4. PSCF

PSCF analysis with transmission height of 1000 m was applied to this study to explore the effects of long-distance transport of atmospheric pollutants on the study area. The results of the PSCF analysis showed that the PAHs and NPAHs mainly originated from

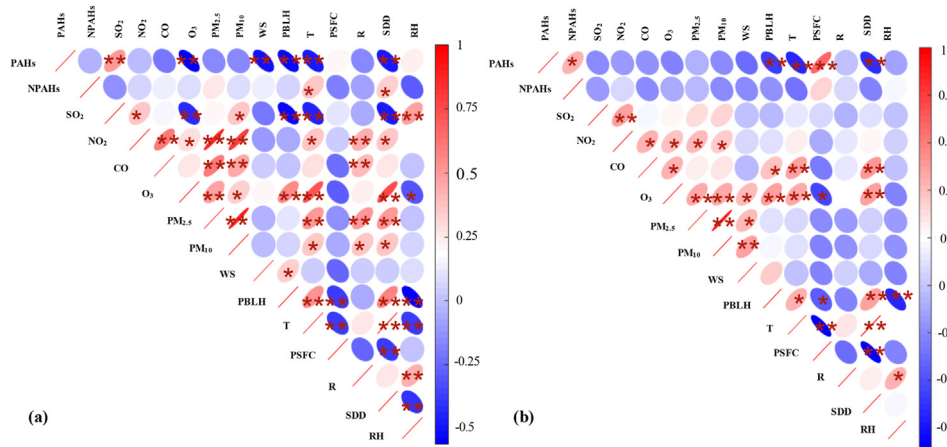


Fig. 2. Correlation among PAHs, NPAHs, atmospheric pollutants and meteorological conditions: (a) heating period and (b) non-heating period. Note: Pearson correlation method is used for the correlation matrix. Each significance level is related to a symbol: p-values (0.01, 0.05) and corresponding symbols (** and *). Abbreviations in the diagram: WS-wind speed; PBLH- mixed layer height; T-average temperature; PSFC-surface pressure; R-daily rainfall; SDD-solar radiation; RH-relative humidity.

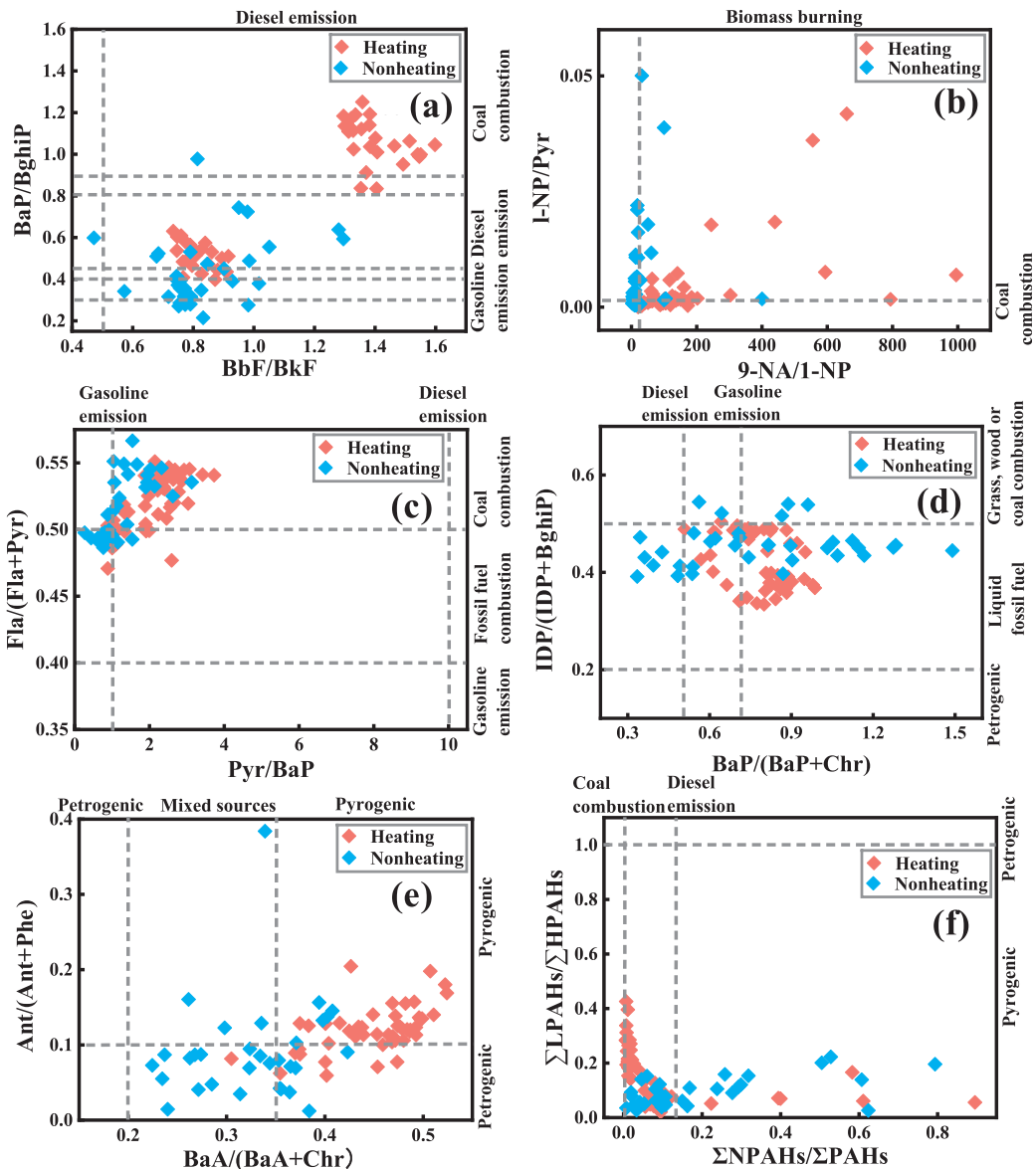


Fig. 3. Bivariate plots of the diagnostic ratios in this work; (a) BaP/BghiP vs. BbF/BkF; (b) 1-NP/Py vs. 9-NA/1-NP; (c) \sum LPAHs/ \sum HPAHs vs. \sum NPAHs/ \sum PAHs; (d) Fla/(Fla + Pyr) vs. Pyr/BaP; (e) IDP/(IDP + BghiP) vs. BaP/(BaP + Chr) and (f) Ant/(Ant + Phe) vs. BaA/(BaA + Chr).

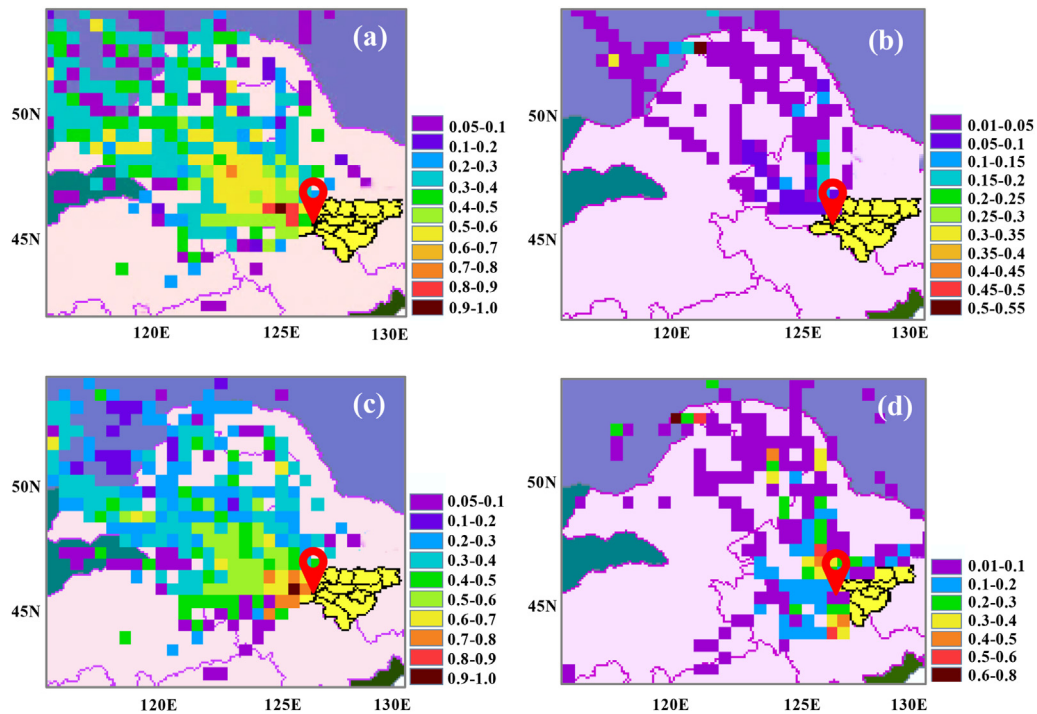


Fig. 4. The results of PSCF analysis of (a) PAHs during the heating period, (b) PAHs in the non-heating period, (c) NPAHs in the heating period, and (d) NPAHs in the non-heating period in Harbin.

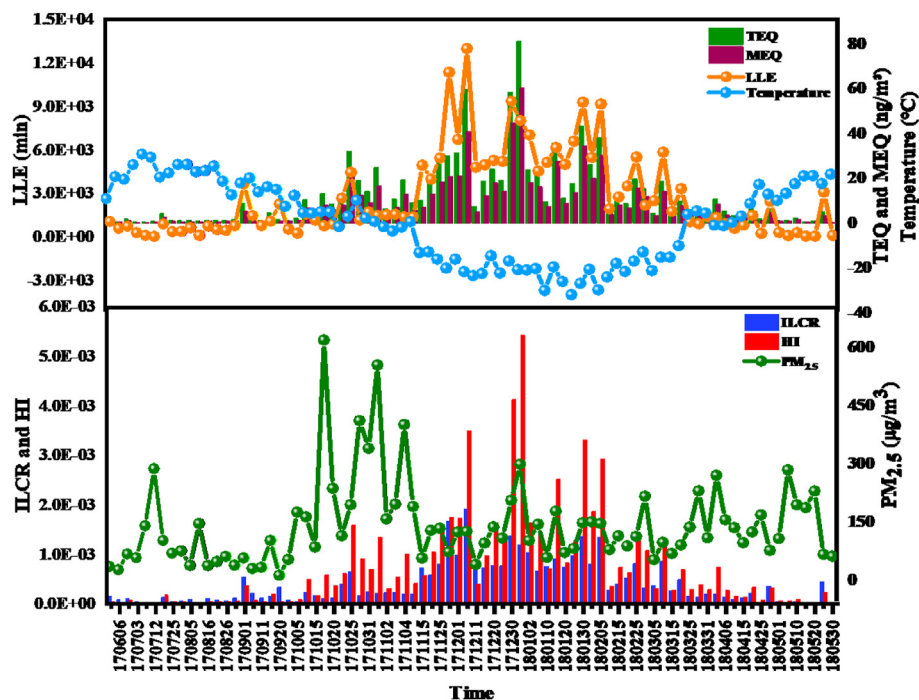


Fig. 5. Temporal variation of $PM_{2.5}$ concentration and health risks in Harbin during the sampling periods.

the northwest of Harbin, and the source regions were similar in heating and non-heating period (Fig. 4). This might be related to emissions from the oil and petrochemical industries in Daqing, China's largest oilfield city in the northwest of Harbin. Compared

with PAHs in the non-heating period, the source regions of NPAHs during the non-heating period were more extensive. This might be related to meteorological conditions including high temperature, extreme solar radiation, excessive mixed layer height and strong

wind, which contributed to the secondary formation and the long-distance transportation of NPAHs in the atmosphere.

3.6. Cancer risk assessment

The limited numbers of species have TEF and MEF values among the PAHs and NPAHs investigated in this study resulting in only a part of the total toxicological picture being shown. The total carcinogenic equivalent toxicity (Σ TEQ) with an average of 9.19 ng/m³ (range from 0.218 to 60.6 ng/m³) was predominantly contributed by PAHs and was higher than the WHO standard value of 1 ng/m³ (Ventafridda et al., 1987) (Table S7). Of note, Σ NPAHs concentration accounted for 1.54% of the Σ PAHs + NPAHs concentration, while Σ TEQ of NPAHs accounted for 5.88% of the total Σ TEQ, indicating the high toxicity of NPAHs. The total mutagenic equivalent toxicity (Σ MEQ) concentrations ranged from 0.266 to 81.2 ng/m³, with a mean value of 12.1 ng/m³. BaP was a major contributor with a contribution rate of 43.1% (Fig. S6). The Loss of life expectancy (LLE) for the two populations (male adult and female adult) were 53.4–11600 min (mean 2475 min) and 66.3–14400 min (mean 3070 min), respectively (Table S8).

Non-CR assessment via the inhalation exposure route is based on Hazaed Index (HI). The annual HI caused by exposure to the PM_{2.5}-bound 9 PAHs was 7.54E-4, with a trend of male adult > female adult > female adolescent > male adolescent > female children > male children (Table S9). Among the 9 PAHs, BaP was the main contributor, averagely contributing 89.4% to the non-CR (Fig. S7).

The annual incremental lifetime cancer risk (ILCR) from exposure to the PM_{2.5}-bound 16 PAHs and 6 NPAHs via inhalation, ingestion and dermal contact were 4.10E-4, with a trend of female adult > female adolescents > male adult > male adolescents > female children > male children. Based on the potential risk values recommended by US EPA (10E-4–10E-6), the ILCRs for the six population investigated in Harbin exceeded acceptable standards (10E-6), demonstrating the potential cancer risk at this PAHs and NPAHs concentration level. In terms of exposure pathways, ingestion and (1.70E-4) and dermal contact (2.40E-4) were the main pathways leading to ILCRs, which were five orders of magnitude higher than those caused by inhalation (Table S10). A comparison of ILCRs caused by PAHs and NPAHs showed that PAHs were the stronger contributor (91.8%), which was related to high PAHs concentration and the fact that only part of NPAHs was calculated. BaP was the compound with the highest carcinogenic risk among 16 PAHs (averagely contributing 58.7%), followed by IDP and BkF (averagely contributing 8.52% and 8.03%, respectively), while 6-NChr (averagely contributing 8.00%) was the dominated contributor to the ILCRs in 6 NPAHs, especially in summer and straw burning period in autumn, the contribution rate could reach 14.2% and 12.8%, respectively (Fig. S8).

Overall, human health risks from exposure to PM_{2.5}-bound PAHs and NPAHs were higher during the heating period, with Σ TEQ, Σ MEQ, HI, ILCRs being 9.11, 8.21, 11.3 and 4.72 times during the heating period than that during the non-heating period indicating the health hazards of coal burning. Compare the trend of health risk and PM_{2.5}, health risks were highest in winter, while PM_{2.5} concentrations were highest in the straw burning period in autumn (Fig. 5). Although the PM_{2.5} concentration in winter was only 45.4% of that in the straw burning period in autumn, the Σ TEQ, Σ MEQ, HI, ILCRs were 2.23, 1.93, 2.62 and 3.16 times in winter than that in the straw burning period in autumn. This indicated that the human health risk from air pollution is not only dependent on PM_{2.5} pollution levels, but also the concentration and species of toxic compounds accumulated on PM_{2.5}.

4. Conclusion

Pollution characteristics of the PM_{2.5}-bound 16 priority PAHs and 16 NPAHs in this cold northern China megacity were studied. Their occurrence, composition, influencing factors were analyzed, and their health risk was assessed. Results showed that the annual concentration of PM_{2.5} (80.8 μ g/m³) were much higher than the annual average exposure limit for China (35 μ g/m³) and WHO (10 μ g/m³), especially in the straw burning period in autumn (234 μ g/m³). The concentrations of PM_{2.5}-bound PAHs and NPAHs were highest in winter (PAHs concentration in winter: 215 ng/m³) and during the straw burning in autumn (NPAHs concentration during the straw burning in autumn: 24.7 ng/m³), respectively. Compared with other countries and regions, the PM_{2.5}-bound PAHs (other studies: 1.34–111 ng/m³, this work: 86.9 ng/m³) and NPAHs (other studies: 0.152–1.88 ng/m³, this work: 5.48 ng/m³) pollution was quite serious in Harbin. The PAHs were mainly derived from coal combustion and biomass burning during the heating period, while vehicle exhausts were the major contributor of PAHs during the non-heating period. The main sources of NPAHs were direct emission and secondary formation, and the latter contributed more to the non-heating period. The transport analysis of atmospheric pollutants showed that PAHs and NPAHs mainly came from the northwest of the Harbin. The health risk assessment showed that residents in Harbin area suffered from potential cancer risk (annual mean ILCR: 4.10E-4) at these levels of PAHs and NPAHs, especially during the heating period (ILCR: 6.00E-4). At present, there is still a lack of study on PM_{2.5}-bound PAHs and NPAHs pollution and health risk assessment in cold areas of China, and the results of this study have certain reference value for controlling air pollution and understanding carcinogenic risk caused by exposure to air pollution in cold areas. Wearing a mask or minimizing outdoor exposure during the heating period is an effective way to reduce the health risks of human exposure to air pollution. It was recommended that solid fuel combustion could be the crucial atmospheric environmental management target during the heating period. Coal purification and methane production by straw fermentation may be effective control methods.

Declaration of competing interest

The authors declare the following financial interests/personal relationships which may be considered as potential competing interests:

CRedit authorship contribution statement

Lixin Ma: Conceptualization, Methodology, Software, Investigation, Writing - original draft. **Bo Li:** Validation, Formal analysis, Visualization, Software. **Yuping Liu:** Writing - review & editing. **Xiazhong Sun:** Resources, Writing - review & editing, Supervision, Data curation. **Donglei Fu:** Validation, Formal analysis, Visualization. **Shaojing Sun:** Resources, Writing - review & editing, Supervision, Data curation. **Samit Thapa:** Writing - original draft. **Jialu Geng:** Investigation. **Hong Qi:** Writing - review & editing. **Anping Zhang:** Writing - review & editing. **Chongguo Tian:** Writing - review & editing.

Acknowledgements

This work was supported by National Key R&D Projects of China (No. 2017YFC0212300), the State Key Laboratory of Urban Water

Resource and Environment, Harbin Institute of Technology (No.2018TS01).

Appendix A. Supplementary data

Supplementary data to this article can be found online at <https://doi.org/10.1016/j.jclepro.2020.121673>.

Unlisted references

Lin et al., 2015; CIMISS-China Meteorological Data Service Center, 2005; Lin et al., 2015;.

References

- Akyüz, M., Çabuk, H., 2010. Gas-particle partitioning and seasonal variation of polycyclic aromatic hydrocarbons in the atmosphere of Zonguldak, Turkey. *Sci. Total Environ.* 408, 5550–5558.
- Albinet, A., Leoz-Garziandia, E., Budzinski, H., et al., 2007. Polycyclic aromatic hydrocarbons (PAHs), nitrated PAHs and oxygenated PAHs in ambient air of the Marseilles area (South of France): concentrations and sources. *Sci. Total Environ.* 384, 280–292.
- Chitranshi, S., Sharma, S.P., Dey, S., 2015. Spatio-temporal variations in the estimation of PM10 from MODIS-derived aerosol optical depth for the urban areas in the Central Indo-Gangetic Plain. *Meteorol. Atmos. Phys.* 127, 107–121.
- Chuesaard, T., Chetiyankornkul, T., Kameda, T., et al., 2014. Influence of biomass burning on the levels of atmospheric polycyclic aromatic hydrocarbons and their nitro derivatives in Chiang Mai, Thailand. *Aerosol Air Qual. Res.* 14, 1247–1257.
- CIMISS-China Meteorological Data Service Center, 2005. <http://data.cma.cn> accessed 10 June 2019.
- Egide, K., Nagato, E.G., Bizuru, E., et al., 2018. Characterization and risk assessment of atmospheric PM2.5 and PM10 particulate-bound PAHs and NPAHs in Rwanda, Central-East Africa. *Environ. Sci. Technol.* 52, 12179–12187.
- Hanedar, A., Alp, K., Kaynak, B., et al., 2014. Toxicity evaluation and source apportionment of polycyclic aromatic hydrocarbons (PAHs) at three stations in Istanbul, Turkey. *Sci. Total Environ.* 488–489, 437–446.
- He, L., Hu, M., Zhang, Y., et al., 2008. Fine particle emissions from on-road vehicles in the Zhujiang Tunnel, China. *Environ. Sci. Technol.* 42, 4461–4466.
- Jariyasopit, N., Zimmermann, K., Schrlau, J., et al., 2014. Heterogeneous reactions of particulate matter-bound PAHs and NPAHs with NO3/N2O5, OH radicals, and O3 under simulated long-range atmospheric transport conditions: reactivity and mutagenicity. *Environ. Sci. Technol.* 48 (17), 10155–10164.
- Li, J., Yang, L., Gao, Y., et al., 2019. Seasonal variations of NPAHs and OPAHs in PM2.5 at heavily polluted urban and suburban sites in North China: concentrations, molecular compositions, cancer risk assessments and sources. *Ecotoxicol. Environ. Saf.* 178, 58–65.
- Lin, Y., Ma, Y., Qiu, X., et al., 2015. Sources, transformation, and health implications of PAHs and their nitrated, hydroxylated, and oxygenated derivatives in PM2.5 in Beijing. *J. Geophys. Res. Atmos.* 120 (14), 7219–7228.
- Ma, Y., Cheng, Y., Qiu, X., et al., 2016. A quantitative assessment of source contributions to fine particulate matter (PM2.5)-bound polycyclic aromatic hydrocarbons (PAHs) and their nitrated and hydroxylated derivatives in Hong Kong. *Environ. Pollut.* 219, 742–749.
- Mabahwi, N.A.B., Leh, O.L.H., Omar, D., 2014. Human health and wellbeing: human health effect of air pollution. *Procedia Soc. Behav. Sci.* 153, 221–229.
- Mugica-Alvarez, V., Santiago-de la Rosa, N., Figueroa-Lara, J., et al., 2015. Emissions of PAHs derived from sugarcane burning and processing in Chiapas and Morelos Mexico. *Sci. Total Environ.* 527, 474–482.
- Nassar, H.F., Tang, N., Kameda, T., et al., 2011. Atmospheric concentrations of polycyclic aromatic hydrocarbons and selected nitrated derivatives in Greater Cairo, Egypt. *Atmos. Environ.* 45, 7352–7359.
- Pietrogrande, M.C., Abbaszade, G., Schnelle-Kreis, J., et al., 2011. Seasonal variation and source estimation of organic compounds in urban aerosol of Augsburg, Germany. *Environ. Pollut.* 159, 1861–1868.
- Querol, X., Alastuey, A., Viana, M., et al., 2004. Speciation and origin of PM10 and PM2.5 in Spain. *J. Aerosol Sci.* 35 (9), 1151–1172.
- Rajput, P., Sarin, M.M., Rengarajan, R., et al., 2011. Atmospheric polycyclic aromatic hydrocarbons (PAHs) from post-harvest biomass burning emissions in the Indo-Gangetic Plain: isomer ratios and temporal trends. *Atmos. Environ.* 45 (37), 6732–6740.
- Ratcliff, M.A., Dane, A.J., Williams, A., et al., 2010. Diesel particle filter and fuel effects on heavy-duty diesel engine emissions. *Environ. Sci. Technol.* 44, 8343–8349.
- Ravindra, K., Sokhi, R., Van Grieken, R., 2008. Atmospheric polycyclic aromatic hydrocarbons: source attribution, emission factors and regulation. *Atmos. Environ.* 42 (13), 2895–2921.
- Ringuet, J., Albinet, A., Leoz-Garziandia, E., et al., 2012. Diurnal/nocturnal concentrations and sources of particulate-bound PAHs, OPAHs and NPAHs at traffic and suburban sites in the region of Paris (France). *Sci. Total Environ.* 437, 297–305.
- Samet, J.M., Dominici, F., Currier, I., et al., 2000. Fine particulate air pollution and mortality in 20 U.S. cities, 1987–1994. *N. Engl. J. Med.* 343, 1742–1749.
- Santos, L.O., Santos, A.G., de Andrade, J.B., 2018. Methodology to examine polycyclic aromatic hydrocarbons (PAHs) nitrated PAHs and oxygenated PAHs in sediments of the Paraguaçu River (Bahia, Brazil). *Mar. Pollut. Bull.* 136, 248–256.
- Sarigiannis, D.A., Karakitsios, S.P., Zikopoulos, D., et al., 2015. Lung cancer risk from PAHs emitted from biomass combustion. *Environ. Res.* 137, 147–156.
- Sevimoglu, O., Rogge, W.F., 2016. Seasonal size-segregated PM10 and PAH concentrations in a rural area of sugarcane agriculture versus a coastal urban area in Southeastern Florida, USA. *Particulology* 28, 52–59.
- Singh, D., Gadi, R., Mandal, T., et al., 2013. Emissions estimates of PAH from biomass fuels used in rural sector of Indo-Gangetic Plains of India. *Atmos. Environ.* 68, 120–126.
- Slezakova, K., Castro, D., Delerue-Matos, C., et al., 2013. Impact of vehicular traffic emissions on particulate-bound PAHs: levels and associated health risks. *Atmos. Res.* 127, 141–147.
- Sofowote, U.M., McCarry, B.E., Marvin, C.H., 2008. Source apportionment of PAH in Hamilton Harbour suspended sediments: comparison of two factor analysis methods. *Environ. Sci. Technol.* 42, 6007–6014.
- Valle-Hernández, B.L., Mugica-Alvarez, V., Salinas-Talavera, E., et al., 2010. Temporal variation of nitro-polycyclic aromatic hydrocarbons in PM10 and PM2.5 collected in Northern Mexico City. *Sci. Total Environ.* 408, 5429–5438.
- Ventafredda, V., Tamburini, M., Caraceni, A., et al., 1987. A validation study of the WHO method for cancer pain relief. *Cancer* 59, 850–856.
- Wang, J., Geng, N., Xu, Y., et al., 2014. PAHs in PM2.5 in Zhengzhou: concentration, carcinogenic risk analysis, and source apportionment. *Environ. Monit. Assess.* 186, 7461–7473.
- Wang, W., Jariyasopit, N., Schrlau, J., et al., 2011. Concentration and photochemistry of PAHs, n-PAH, and PAH and toxicity of PM2.5 during the Beijing Olympic games. *Environ. Sci. Technol.* 45, 6887–6895.
- Yang, B., Zhou, L.L., Xue, N.D., et al., 2013. Source apportionment of polycyclic aromatic hydrocarbons in soils of Huanghuai Plain, China: comparison of three receptor models. *Sci. Total Environ.* 443, 31–39.
- Yin, H., Xu, L., 2018. Comparative study of PM10/PM2.5-bound PAHs in downtown Beijing, China: concentrations, sources, and health risks. *J. Clean. Prod.* 177, 674–683.
- Zhan, J., Yang, Y., Liu, D., et al., 2012. The research progress of nitrated polycyclic aromatic hydrocarbons in the atmosphere (in Chinese). *Sci. Sin.: Terra* 42, 1–9.
- Zhang, J., Wang, J., Hua, P., et al., 2015. The qualitative and quantitative source apportionment of polycyclic aromatic hydrocarbons in size dependent road deposited sediment. *Sci. Total Environ.* 505, 90–101.
- Zhang, Y., Schauer, J.J., Zhang, Y., et al., 2008. Characteristics of particulate carbon emissions from realworld Chinese coal combustion. *Environ. Sci. Technol.* 42, 5068–5073.
- Zimmermann, K., Jariyasopit, N., Simonich, S.L.M., et al., 2013. Formation of nitro-PAHs from the heterogeneous reaction of ambient particle-bound PAHs with N2O5/NO3/NO2. *Environ. Sci. Technol.* 47, 8434–8442.